Desalination and Water Treatment
www.deswater.com

doi: 10.1080/19443994.2016.1147380

57 (2016) 25317–25328
November

Taylor & Francis
Taylor & Francis Group

Application of response surface methodology for modeling and optimization of trichloroacetic acid and turbidity removal using potassium ferrate(VI)

Hassan Aslani[a], Ramin Nabizadeh[a,c], Simin Nasseri[a,b,*], Alireza Mesdaghinia[a], Mahmood Alimohammadi[a], Amir Hossein Mahvi[a,d], Noushin Rastkari[c], Shahrokh Nazmara[a]

[a]*School of Public Health, Department of Environmental Health Engineering, Tehran University of Medical Sciences, Tehran, Iran, emails: Aslani.ha@gmail.com (H. Aslani), Rnabizadeh@tums.ac.ir (R. Nabizadeh), naserise@tums.ac.ir (S. Nasseri), Mesdaghini@sina.tums.ac.ir (A. Mesdaghinia), M_alimohammadi@tums.ac.ir (M. Alimohammadi), Ahmahvi@yahoo.com (A.H. Mahvi), Snazmara@gmail.com (S. Nazmara)*
[b]*Center for Water Quality Research, Institute for Environmental Research, Tehran University of Medical Sciences, Tehran, Iran*
[c]*Center for Air Pollution Research, Institute for Environmental Research, Tehran University of Medical Sciences, Tehran, Iran email: N_rastkari@yahoo.com (N. Rastkari)*
[d]*Center for Solid Waste Research, Institute for Environmental Research, Tehran University of Medical Sciences, Tehran, Iran*

Received 11 October 2015; Accepted 20 January 2016

ABSTRACT

Coagulation/flocculation and oxidation are two of the main processes in treating colloidal and organic substances. Potassium ferrate(VI), a multipurpose chemical, is used in water treatment plants as coagulant and oxidant. In this study, ferrate(VI) was evaluated for the degradation of trichloroacetic acid and turbidity removal in synthetic water. The effects of five independent variables, initial pH of solution (3–9), ferrate(VI) dosage (1–10 mg L^{-1}), contact time (5–60 min), trichloroacetic acid concentration (100–1,000 μg L^{-1}), and initial turbidity (1–10 NTU) were investigated and the process was optimized by means of response surface methodology. Trichloroacetic acid and turbidity removal efficiencies were considered as the process responses. The highest efficiency achieved for trichloroacetic acid removal was 24%, while for turbidity the maximum removal efficiency was in the range 85–95%. The optimum conditions for initial turbidity, pH, and ferrate dosage were 8.89 NTU, 3, and 4.26 mg L^{-1} as Fe, respectively. Experimentally obtained 89% turbidity removal in the optimum condition confirmed the results predicted by the model. Therefore, it can be concluded that ferrate(VI) can be effectively used in colloidal substances removal, while it is not successful enough in trichloroacetic acid decomposition.

Keywords: Trichloroacetic acid; RSM; Optimization; Ferrate(VI); Coagulation

1. Introduction

Trichloroacetic acid (TCAA) is one of the resistant and main disinfection byproducts which is produced in chlorination step in water and wastewater treatment plants. Due to the fact that TCAA is a toxic and carcinogenic compound, and also because of its widespread presence in the environment, more attention is paid in recent years by both authorities and researchers

---

*Corresponding author.

[1], and it has been shown that human exposure is possible not only through ingestion but also through dermal contact or inhalation [2]. Toxicological effect of TCAA has been reported in literature [3,4], and according to its carcinogenic potential USEPA has classified TCAA as a possible human carcinogen (group C) [5].

In the chemical coagulation/flocculation process both physical and chemical properties of colloidal or suspended particles are altered in a way that agglomeration and production of larger particles is enhanced, and they can be settled out of solution by gravity [6–10]. Some traditional compounds such as aluminum sulfate (Alum), aluminum chloride, and ferric chloride have been used to change the surface charge of colloids and promote the agglomeration and/or enmeshment of smaller particles into larger flocs [11–13]. However, besides their effectiveness on turbidity removal, and aluminum-based coagulants, particularly alum, may release higher Al^{3+} concentration to the treated water. The occurrence of Al^{3+} in treated water has been considered as an undesirable aspect of treatment practice and it has been associated with several problems such as increased turbidity, affecting disinfection process, and a loss in hydraulic capacity [13]. On the other hand, the ingestion of high concentrations of Al^{3+} is also of concern due it’s possible adverse health effects including Alzheimer disease [14–16].

Regarding the increase of water resources pollution and the stringent standards enacted for drinking water supply and wastewater discharge to achieve treated water qualities, more efficient water treatment chemical reagents need to be considered. Potassium ferrate (VI), K_2FeO_4, has been introduced as a multipurpose agent for coagulation [17,18], disinfection [19], and oxidation [20,21], and is used in water and wastewater treatment of plants. Ferrate(VI) is a strong oxidizing agent which has shown various reduction potentials based on the Eqs. (1) and (2) in acidic and alkaline solutions, respectively [22].

$$FeO_4^{2-} + 8H^+ + 3e^- \leftrightarrow Fe^{3+} + 4H_2O, \quad E^0 = +2.2V \tag{1}$$

$$FeO_4^{2-} + 4H_2O + 3e^- \leftrightarrow Fe^{3+} + 5OH^-, \quad E^0 = +0.72V \tag{2}$$

As shown in Eq. (1), ferrate(IV) is a powerful oxidant, especially in acidic conditions, and its redox potential (2.2 V) is higher than O_3 (2.07 V), Cl_2 (1.35 V), and H_2O_2 (1.77 V). A good number of investigations have been conducted in which ferrate(VI) has been considered as a potent chemical in order to oxidize organic impurities [23–26]. Moreover, its final byproduct Fe (III) is a promising coagulant that can efficiently remove colloidal particles from aquatic environments. Turbidity removal performance of ferrate has been compared with other iron salts such as ferrous sulfate and ferric nitrate, reporting that the final turbidity in water samples treated by ferrate(VI) was lower than the samples treated using $FeSO_4{\cdot}7H_2O$ and $Fe(NO_3)_3$ [22,27]. Another advantage of ferrate(VI) in comparison to other iron and aluminum salts is that it can destabilize colloidal particles in >1 min, while iron and aluminum-based coagulants need about 30 min mixing time [22].

To date, studies have reported ferrate(VI) as a promising coagulant in water and wastewater treatment [28–30]. In all of the studies using ferrate as coagulant, conventional and classical experiments were tested. In the classical method of experimentation one factor is changed, while others are fixed, which requires many experimental runs. Moreover, the classical approach is labor-intensive and time-consuming, and ignores interaction effects between the variables; so the optimization is not as precise as expected [31]. Hence, the response surface methodology (RSM) may be considered as an efficient way to deal with the limitations of the conventional method. RSM involves statistical design of experiments in which all factors are varied simultaneously, and can be a useful technique for optimization, analysis, and modeling the effects of multiple variables and their responses [32].

The objective of this study was to investigate ferrate(VI) as an alternative oxidant and coagulant for TCAA and turbidity removal, respectively. RSM using central composite design (CCD) was applied to develop mathematical and statistical correlation between initial pH, ferrate dosage, contact time, initial TCAA concentration and turbidity for TCAA, and turbidity removal efficiency.

2. Materials and methods

2.1. Materials

Potassium ferrate(VI) with a labeled purity of more than 92% was obtained from BOC Science (NY, USA), and used without further purification. Tap water was used to make artificial turbidity using bentonite (Kimya-Pazhouh Co., Iran). TCAA, methyl tert-butyl ether (MTBE), 1,2,3 trichloropropane, and 2-bromobutanoic acid, all in analytical grade, were purchased from Sigma–Aldrich. Analytical pure methanol, sodium sulfate, sodium bicarbonate, sulfuric acid, hydrochloric acid, and sodium hydroxide were provided by Merck Co. (Germany).

2.2. Sample preparation and analysis

In order to provide desired turbidities, synthetic turbid water was daily prepared using laboratory grade bentonite in 2L of tap water. Using this turbid water the aqueous solution of desired TCAA concentration was prepared from a 5-g/L stock solution. Before adding TCAA to the tap water, residual chlorine was quenched using 3% sodium thiosulfate. Turbidity was measured with a 2100AN Hatch Turbidimeter.

Trichloroacetic acid was measured by liquid-liquid extraction, methylation, and derivatization following the USEPA method 552.3 [33], and using a GC-ECD (Varian CP 3800, United States) equipped with a DB-1701 capillary column (30 m × 0.25 mm × 0.25 mL, Optima, Germany). Operation conditions of GC were: injector temperature (250℃); and detector temperature (290℃); and the temperature program of the oven was arranged as follows: started at 40℃ (held for 10 min), ramped to 65℃ with 2.5℃/min, set at 10℃/min to 85℃, set at 20℃/min to 205℃, and finally held isothermally for 7 min.

2.3. Jar test experiments

The visible spectrum of Fe(VI) in 6-M NaOH solution is shown in Fig. S1 (Supplementary Figure), which shows the maximum absorption at 510 nm. Ferrate(VI) concentration was determined by UV–vis spectrometry (PerkinElmer Lambda 25 Spectrometer, USA), and a molar absorption coefficient of 1,150 M^{-1} cm^{-1} was used for the calculations [34]. To minimize colloidal ferric oxide interference, base line correction was made in 385 nm [35]. Ferrate(VI) stock solution at 1,000 mg L^{-1} as Fe, was freshly prepared just 5 min before the experiments by adding solid samples of K_2FeO_4 to doubled distilled and used within 10 min in order to minimize self-decomposition. A standard six paddle jar test (Lovibond, USA) was used for coagulation and flocculation process. The coagulation/flocculation and oxidation experiments were carried out using 500-mL sample volume in 1L beakers. After the addition of coagulant (i.e. ferrate (VI)), with a determined dosage, pH was adjusted to 3–9 by adding 0.3 mol L^{-1} of HCl or NaOH solutions. The sample was immediately stirred at a constant speed of 300 rpm for 1 min, followed by a slow mixing at 35 rpm for 10 min; then, a settlement for 15 min was performed. Samples were taken from about 2 cm below water surface using a 100 mL pipet [36]. At least 20 mL sample was required for residual turbidity measurement and 40 mL to determine residual TCAA concentration.

2.4. Experimental design

CCD was used to study turbidity and TCAA removal using potassium ferrate. RSM was used for the determination of combined effects of initial TCAA concentration (X_1), pH (X_2), ferrate(VI) dosage (X_3), contact time (X_4), and initial turbidity (X_5) on the turbidity removal (Y_1) and TCAA decomposition (Y_2). The study was divided into two different phases named as preliminary and main study. In the former, in order to determine the true range of factors, and also their effects on turbidity and TCAA removal, a full factor design considering five above-mentioned controllable variables, was carried out. The actual and coded levels of the design are shown in Table 1. Totally, 49 experiments were designed using 2*k* and 17 replicates in the center point, where *k* was the number of variables. Dependent variables of the process including removal efficiency of turbidity (Y_1), and TCAA (Y_2) were served as output responses.

After determining which factor affects the responses, the second phase, i.e. main study, started using effective factors, and removing the others. Table 2 shows the design parameters and values for the 2nd phase of the study. An orthogonal CCD in two cube and star blocks was designed, and in total 29 experiments were carried out, consisting of 15 center points, $2^3 = 8$ design points, and $2 \times 3 = 6$ axial

Table 1
Real and coded values of independent variables used for experimental design in phase 1

		Coded levels		
		−1	0	1
Variable	Symbol	Real values		
TCAA (μg L^{-1})	X_1	100	550	1,000
pH	X_2	3	6	9
Ferrate (mg L^{-1})	X_3	5	10	15
Time (min)	X_4	5	32.5	60
Turbidity (NTU)	X_5	1	5.5	10

Table 2
Real and coded values of independent variables used for experimental design in the 2nd phase

		Coded levels				
		−α	−1	0	1	α
Variables	Symbol	Real values				
Turbidity (NTU)	X_1	1	2.82	5.5	8.18	10
pH	X_2	3	4.21	6	7.79	9
Ferrate (mg/L)	X_3	1	2.82	5.5	8.18	10

points. The selected independent factors were coded based on Eq. (3):

$$x_i = \frac{(X_i - X_0)}{\Delta X} \tag{3}$$

where X_i is a dimensionless coded value of the ith independent variable, X_0 is the center point value of X_i, and ΔX is the step change value. A quadratic (second order) model as shown in Eq. (4) was applied to approximate the interaction between turbidity removal as response (Y) and three independent variables:

$$Y = b_0 + \sum_{i=1}^{k} b_i X_i + \sum_{i=1}^{k} b_{ii} X_i^2 + \sum_{i=1}^{k-1} \sum_{j=2}^{k} b_{ij} X_i X_j + c \tag{4}$$

where Y represents the dependent variable, b_0 is a constant value, b_i, b_{ii}, and b_{ij} refer to the regression coefficient for linear, second order, and interactive effects, respectively, X_i and X_j are the independent variables, and c denotes the error of prediction. The above-mentioned CCD analysis, and the related statistical analysis, such as ANOVA, F-test, and t-test were obtained using *R* software for windows (version 3.0.3: 6 March 2014).

3. Results and discussion

3.1. Preliminary study

This phase was conducted to find out the effective variables and their proper range in our study. In order to determine which variable and how it affects the response variables, effect plots were prepared based on the results presented in Table 3. Effect plots of independent variables on turbidity and TCAA removal are depicted in Fig. 1(a) and (b), respectively. It is clear that pH and initial turbidity significantly affected turbidity removal, while contact time and TCAA concentration did not show any considerable effects. Ferrate(VI) concentration showed little effect, although ferrate(VI) coagulation performance has been proved in the previous studies [17,18,27,37], therefore it can be inferred that ferrate(VI) concentration range was not properly chosen in this phase, and needed to be changed.

For TCAA removal it is obvious from Fig. 1(b) that TCAA initial concentration was the most important factor which negatively affects its removal efficiency; in

Table 3
Preliminary full factor design for TCAA and turbidity removal by Ferrate(VI)

Run no.	X_1	X_2	X_3	X_4	X_5	Y_1	Y_2	Run no.	X_1	X_2	X_3	X_4	X_5	Y_1	Y_2
1	1,000	3	5	5	10	0	5.43	26	1,000	9	15	60	1	5	15.9
2	550	6	10	32.5	5.5	88.18	34.54	27	550	6	10	32.5	5.5	84.55	28.73
3	1,000	3	15	60	1	13	11.28	28	100	3	15	60	1	0	22.40
4	550	6	10	32.5	5.5	90.36	23.81	29	100	3	15	5	1	0	19.70
5	1,000	3	15	5	1	0	10.8	30	550	6	10	32.5	5.5	78.18	20.36
6	550	6	10	32.5	5.5	92.36	22.9	31	1,000	9	5	60	1	0	8.14
7	100	9	5	5	10	0	27	32	100	9	15	60	1	0	14.60
8	1,000	9	5	60	10	0	9.84	33	550	6	10	32.5	5.5	92.55	37.95
9	100	9	15	60	10	0	24.1	34	1,000	3	5	5	1	5	3.70
10	1,000	3	15	5	10	90	4.3	35	550	6	10	32.5	5.5	91.82	11.45
11	550	6	10	32.5	5.5	92.55	25.09	36	100	3	15	60	10	92.4	11.00
12	1,000	9	5	5	1	0	5.2	37	1,000	9	15	60	10	5	18.30
13	550	6	10	32.5	5.5	86	25.81	38	1,000	9	15	5	1	9	6.22
14	1,000	9	5	5	10	0	6.6	39	1,000	3	15	60	10	95.4	8.20
15	100	9	5	5	1	2	6.3	40	100	3	5	60	10	85.2	9.00
16	550	6	10	32.5	5.5	90	42.72	41	100	9	5	60	10	0	7.00
17	100	3	15	5	10	93.6	9	42	100	3	5	60	1	38	2.00
18	550	6	10	32.5	5.5	88.18	25.81	43	100	3	5	5	1	0	22.40
19	550	6	10	32.5	5.5	91.82	21.45	44	1,000	3	5	60	1	43	4.68
20	100	9	15	5	1	0	10.5	45	100	9	15	5	10	4.7	12.20
21	550	6	10	32.5	5.5	84.36	14.9	46	550	6	10	32.5	5.5	89.09	36.67
22	100	3	5	5	10	80.2	14	47	550	6	10	32.5	5.5	84.55	22.54
23	550	6	10	32.5	5.5	80	20.72	48	1,000	3	5	60	10	94.6	0.84
24	1,000	9	15	5	10	71	7.95	49	550	6	10	32.5	5.5	82.55	25.09
25	100	9	5	60	1	6	12.3								

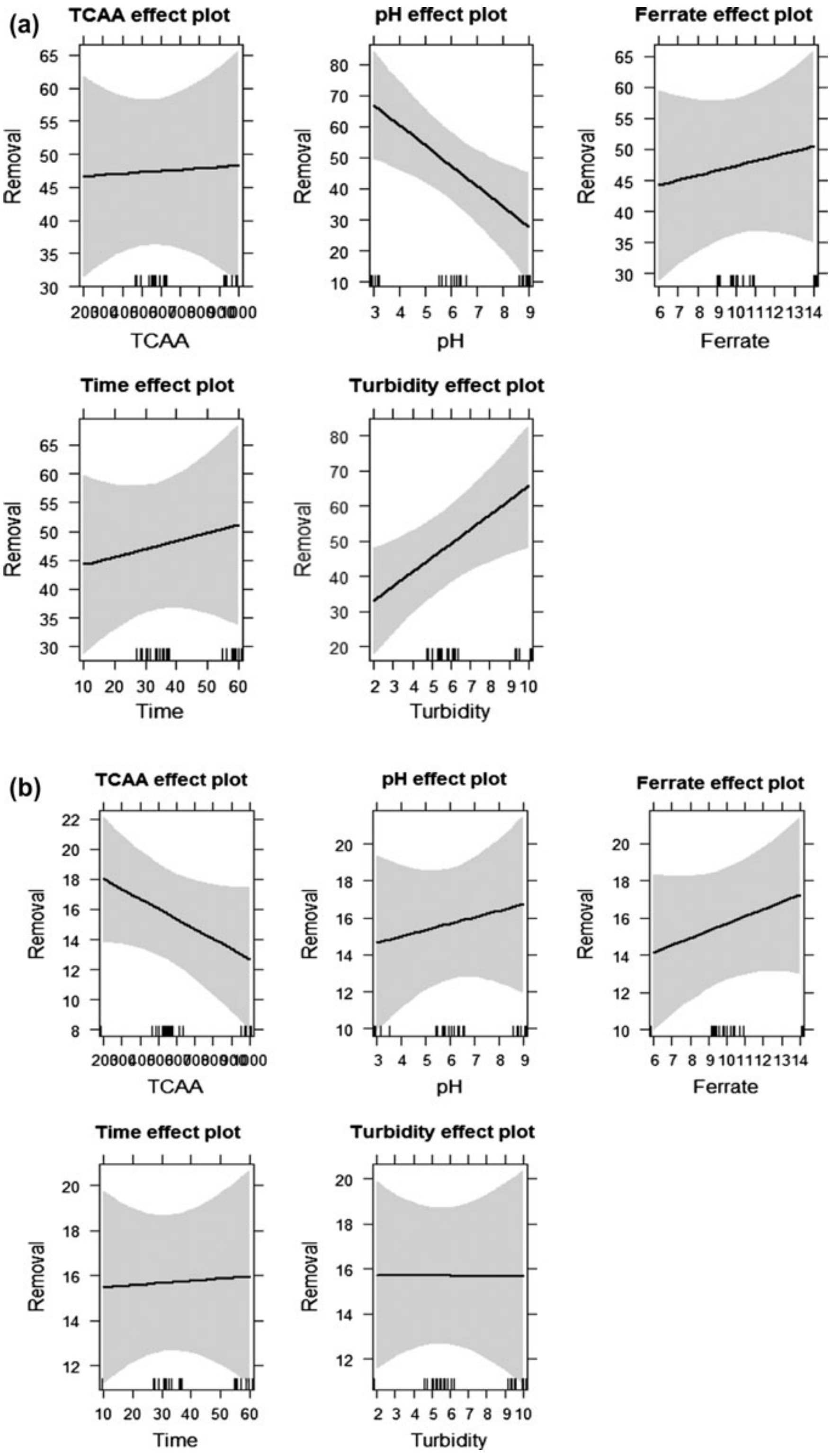

Fig. 1. Effect plot of the independent variables on (a) turbidity removal and (b) TCAA removal.

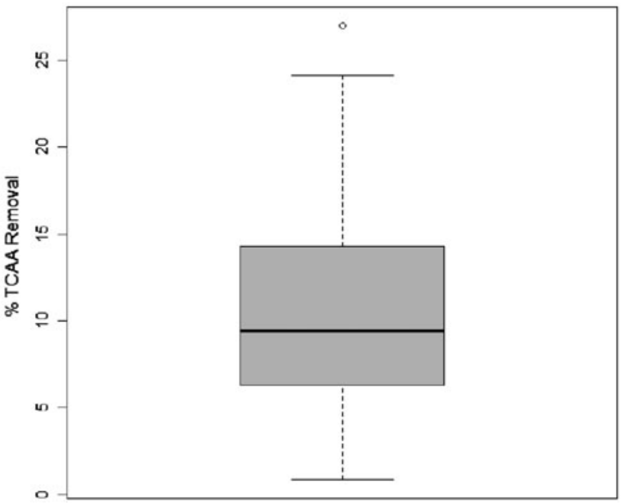

Fig. 2. Box and whisker plot of TCAA removal efficiency using ferrate(VI). The bottom of the box is the 25th percentile and the top is the 75th. The whiskers represent the maximum and minimum for treatment process.

other words the removal percentage was declined by increasing TCAA initial concentration, and ferrate(VI) showed negligible effect; moreover, other parameters, (time, pH, and turbidity) could not affect its removal. The extent of TCAA removal by ferrate(VI) is shown in Fig. 2. This figure indicates that TCAA removal was skewed toward higher values, but confirms that in 75% of the cases the removal efficiency was lower than 15%. The highest TCAA removal percentage achieved was 24% and the median was 9%, which indicates that ferrate(VI), when used alone, is not promising for TCAA degradation. However, the 24% removal efficiency achieved in this study was higher than the efficiency reported by Wang et al. which showed that using single UV or O_3 was not successful to decompose TCAA in 30 min reaction time [38]. Furthermore, it can be inferred from Table 3 that, the higher TCAA removal efficiencies were achieved in the acidic pH range when the initial turbidity was higher than 5 NTU. It is obvious that higher initial turbidities could affect TCAA removal, positively. As TCAA removal is negligible in lower turbidities (see Table 3), it seems that either physical adsorption or TCAA entrapped by the $Fe(OH)_3$ flocs were two possible mechanisms. On the other hand, as ferrate(VI) could achieve reasonable performance at lower doses, it can be interesting to water industries as this will reduce the chemical consumptions, sludge production, and ultimately save the operating cost [28].

Results of the developed model for TCAA removal and its coefficients are shown in Table 4. Regression analysis of the model confirms the results obtained from effect plots. It is clear that TCAA initial concentration was the only variable affecting the model significantly ($p = 0.00837$). Multiple R^2, R^2_{adj}, and p-value calculated for the model were 0.32, 0.19, and 0.055, respectively, which indicate a non-significant model.

Results of regression analysis for turbidity removal are shown in Table 5. As mentioned above it can be seen that in the linear model terms, the removal

Table 4
Regression analysis for the linear model of TCAA removal

Model term	Coefficient estimate	Std. error	*t*-value	*p*-value
Intercept	10.965	1.052	10.417	9×10^{-11}
TCAA	−3.003	1.052	−2.854	0.00837
pH	1.044	1.052	0.99	0.33
Ferrate	1.9381	1.052	1.841	0.077
Time	0.2587	1.052	0.246	0.8077
Turbidity	−0.0427	1.052	−0.04	0.968

Table 5
Regression analysis for the linear model of turbidity removal

Model term	Coefficient estimate	Std. error	*t*-value	*p*-value
Intercept	47.35083	5.433	8.715	4.7×10^{-11}
TCAA	0.90312	6.723	0.134	0.8937
pH	−19.61563	6.723	−2.917	0.0055
Ferrate	3.90937	6.723	0.581	0.5639
Time	3.81563	6.723	0.567	0.5733
Turbidity	18.47188	6.723	2.747	0.00874

efficiency was significantly affected by pH (X_2) and initial turbidity (X_5) with p-values equal to 0.0055 and 0.00874, respectively. It should be noted that pH showed antagonistic, while initial turbidity had synergistic effect. Multiple R^2, R^2_{adj}, and p-value for the turbidity removal are 0.28, 0.196, and 0.012, respectively. It can be seen that although R^2 and R^2_{adj} are not promising, but the model is significant, inferring that it could be improved by changing the range of variables.

3.2. Main study

Based on the results obtained in the preliminary study, it was clear that ferrate(VI) oxidation potential was not high enough to completely oxidize TCAA, and according to Fig. 1 removal efficiencies were negligible; moreover, TCAA did not drive into or adsorb by the flocs produced in coagulation/flocculation process, in other words no interaction was observed between TCAA and turbidity. Therefore, in this step it was decided to pretermit TCAA from the study, and new experimental design was carried out using effective factors only on turbidity removal (see Table 2).

Detailed design and removal efficiency as a response and predicted values are shown in Table 6. It has been stated that when traditional jar test is replaced by RSM jar test, the operators are not able to identify the optimum conditions as the RSM results need to be analyzed through the optimization process. Therefore, in order to overcome this difficulty it has been suggested that they can use Table 6 results to determine optimum conditions [39]. From Table 6, it can be seen that turbidity removal efficiencies lie between 0 and 85.96%, which was related to runs number 26 and 1, respectively. Moreover, considering runs numbers 4, 8, 12, 13, 21, and 26 which have shown lower removal efficiencies than the others, it is obvious that lower turbidity level and/or higher ferrate(VI) concentration were the main reasons. When these two items (low turbidity and high ferrate concentration) were combined, e.g. run 12, the antagonistic effect was very significant and the removal efficiency decreased dramatically. By direct reading of the RSM Table, run 1 was decided as optimum condition, as it showed the highest removal efficiency, and also because of the pH, which is a very crucial parameter in water treatment plants. Although, some other conditions such as runs 5, 15, and 23 were eligible to be considered as optimum conditions; however, in these cases pH was in acidic range which may cause serious operational difficulties in water treatment processes, and ferrate(VI) dosage was also much higher than run 1, which adversely affects economical feasibility of using ferrate(VI) as it is very expensive in comparison to other coagulants. The conditions for run1 were initial turbidity: 8.18 NTU, pH 7.79, and ferrate dosage of 2.82 mg L^{-1}.

3.3. Development of regression model equation and model analysis

Reduced quadratic model was generated by multiple regression, and summarized in Table 7. According to this table it is obvious that all model terms are significant (p-values < 0.05), so all terms presented in Table 7 could impress model formulation. It is evident from this table that initial turbidity (X_1) and ferrate (VI) dosage (X_3) have synergistic effect on the

Table 6
CCD experimental design for turbidity removal by coagulation/flocculation

Run no.	Turbidity	pH	Ferrate	Removal	Predicted	Run no.	Turbidity	pH	Ferrate	Removal	Predicted
1	8.18 (1)	7.79 (1)	2.82 (−1)	85.94	80.85	16	5.5 (0)	6 (0)	5.5 (0)	68.55	68.54
2	8.18 (1)	7.79 (1)	8.18 (1)	70.05	72.18	17	5.5 (0)	6 (0)	5.5 (0)	72.00	68.54
3	5.5 (0)	6 (0)	5.5 (0)	58.00	68.54	18	5.5 (0)	6 (0)	5.5 (0)	69.82	68.54
4	2.82 (−1)	4.21 (−1)	2.82 (−1)	26.29	33.32	19	10 (α)	6 (0)	5.5 (0)	81.90	84.48
5	8.18 (1)	4.21 (−1)	8.18 (1)	77.87	80.86	20	5.5 (0)	6 (0)	5.5 (0)	63.82	68.54
6	5.5 (0)	6 (0)	5.5 (0)	58.36	68.54	21	5.5 (0)	6 (0)	10 (α)	57.82	47.96
7	5.5 (0)	6 (0)	5.5 (0)	61.45	68.54	22	5.5 (0)	6 (0)	5.5 (0)	70.91	68.54
8	2.82 (−1)	7.79 (1)	2.82 (−1)	26.29	24.64	23	5.5 (0)	3 ($-\alpha$)	5.5 (0)	83.64	75.83
9	5.5 (0)	6 (0)	5.5 (0)	62.18	68.54	24	5.5 (0)	9 (α)	5.5 (0)	63.64	61.24
10	5.5 (0)	6 (0)	5.5 (0)	63.64	68.54	25	5.5 (0)	6 (0)	1 ($-\alpha$)	60.00	62.53
11	5.5 (0)	6 (0)	5.5 (0)	61.82	68.54	26	1 ($-\alpha$)	6 (0)	5.5 (0)	0.00	−9.97
12	2.82 (−1)	7.79 (1)	8.18 (1)	0.78	15.97	27	5.5 (0)	6 (0)	5.5 (0)	73.82	68.54
13	2.82 (−1)	4.21 (−1)	8.18 (1)	19.56	24.65	28	5.5 (0)	6 (0)	5.5 (0)	74.91	68.54
14	5.5 (0)	6 (0)	5.5 (0)	72.55	68.54	29	5.5 (0)	6 (0)	5.5 (0)	81.45	68.54
15	8.18 (1)	4.21 (−1)	2.82 (−1)	85.08	89.53						

Table 7
Regression analysis for the reduced quadratic model

Model term	Coefficient estimate	Std. error	*t*-value	*p*-value
Intercept	−32.2773	1.806	37.545	2.2×10^{-16}
Turbidity (X_1)	27.4875	3.417	−2.13	0.044
pH (X_2)	−2.4317	3.425	−2.127	0.0443
Ferrate (X_3)	5.60368	3.425	13.794	1.3×10^{-12}
Turbidity^2 (X_1^2)	−1.5448	5.098	−2.611	0.0156
Ferrate^2 (X_3^2)	−0.6566	5.098	−6.138	2.9×10^{-6}

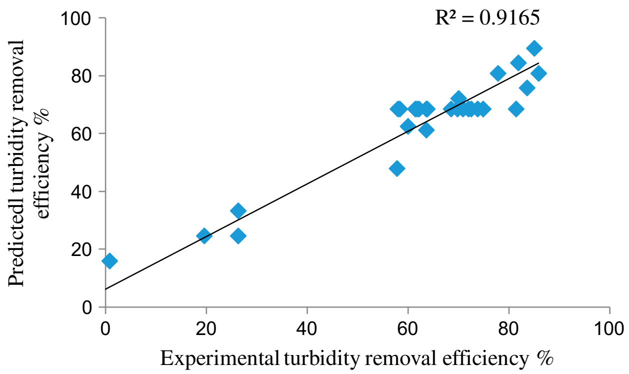

Fig. 3. Experimental turbidity removal vs. predicted removal efficiency.

response prediction by the model, while pH (X_2), X_1^2, and X_3^2 shows antagonistic effect. Turbidity removal efficiency predicted by the model is presented in Table 6. The model is reliable when the response should be predicted by the model and experimental data are obtained in the laboratory correlate linearly, and the points are scattered evenly on a 45° line [40]. Experimental turbidity removal efficiency (%) with those predicted by the model is depicted in Fig. 3. The figure shows good agreement between experimental removal efficiency and the values predicted by the model. Therefore, the model can be used for prediction and optimization [31]. Also, model adequacy can be explained by ANOVA analysis shown in Table 8, as well as using R^2 and R^2_{adj}. The higher *F*-value of 49.49 and accordingly lower *p*-value of 0.000 in Table 8 implies that the second-order polynomial model is statistically significant, in other words the model fitted experimental results well. In addition, the significance of each variable and their interaction is checked by Fisher test. *F*-values of linear and quadratic terms of the model are 66.57 and 23.86, respectively, indicating that the model and the individual coefficients of the model are more significant. The lack of fit *F*-test through comparing residual error to the pure error, especially from the center points, determines data variation around the fitted model and must be insignificant in a well-fitted model [40], the lack of fit value of the model presented in Table 8, i.e. 0.22, indicates the significant correlation between factors and turbidity removal as response [41]. In general, the overall efficiency of the model is explained by R^2, however, it should not be assessed only by this parameter. A high R^2 value close to one and its good agreement with R^2_{adj} is expected, representing satisfactory adjustment between quadratic model and experimental data [40–42]. The R^2 and R^2_{adj} in our study was 0.915 and 0.896, respectively. This means that more than 91.5% data deviation can be explained by the developed model, also R^2_{adj} is in good agreement with R^2_{pred} (see Table 8), implying that significant terms are included in the model [31].

Table 8
Analysis of variance (ANOVA) for the reduced quadratic model

Model formula in RSM (X_1, X_2, X_3)	DF	Sum of squares	Mean square	*F*-value	Probability (P)
First-order response	3	11,308.2	3769.4	66.5724	<0.00001
Pure quadratic response	2	2,702.8	1351.4	23.8673	<0.00001
Residuals	23	1,302.3	56.6	–	–
Lack of fit	9	649.7	72.2	1.5485	–
Pure error	14	652.6	46.6	–	–

Notes: *F*-statistic: 49.49 on 5 and 23 DF, *p*-value: 0.0000, Multiple $R^2 = 0.915$; Adjusted $R^2 = 0.8965$; predicted $R^2 = 0.8496$; Lack of fit: 0.2234.

3.4. Response surface methodology and contour plotting

In order to show the effects of all factors and the interactions clearly, graphical representation of the contour plots, which is developed based on the model coefficients given in Table 6, is shown in Fig. 4. The most important factors affecting turbidity removal efficiency in the coagulation/flocculation process are pH, coagulant dosage, and initial turbidity [41]. In Fig. 4(a), the effects of ferrate(VI) dosage and pH are shown at initial turbidity of 5.5 NTU. Removal efficiency was decreased from 75 to 65% if pH was increased from 3 to 7, keeping ferrate concentration and initial turbidity constant (4 mg L^{-1} and 5.5 NTU, respectively); in other words, removal efficiency increased by decreasing pH. This is expected due to the fact that pH plays an important role in coagulation/flocculation process. pH variations can control both the charge on hydrolysis products and also, precipitation of metal hydroxides [43]. As the surface charges of bentonite clay are anionic, hydrolysis products of the ferrate(VI) (iron hydroxides) can neutralize the negative charges on the collide surface.Therefore, charge neutralization seems to be the most likely mechanism dealing with turbidity removal, and sweeping could be considered as a possible mechanism. On the other hand, with pH decline, protonation processes may lead to the charge density reduction and results in self-aggregation of anionic collide [44], hence less coagulant would be required. According to Fig. 3(a), at lower pH values, less ferrate(VI) dosage was required to obtain a certain turbidity removal efficiency which is in agreement with this theory.

The plot shown in Fig. 4(b) indicates the influence of pH and initial turbidity on the turbidity removal efficiency. Based on the results shown in Fig. 4(b), it is clear that the removal efficiencies in lower turbidities, e.g. in the range of 1–5 NTU, was laid between 0 and 60%, and also pH of the solution did not affect removal efficiency in this range. On the other hand, it can be seen that higher removal efficiencies were achieved when the initial turbidity was higher than 5 NTU. Generally, higher turbidity removal efficiency has been reported in raw water samples with higher initial turbidity [45]. As mentioned for ferrate and pH interaction, in the turbidity range 8–10 NTU, removal efficiency was decreased with increasing pH from 3 to 9.

The interaction effects of ferrate(VI) dosage (X_3) and initial turbidity (X_1) are shown in Fig. 4(c), when the pH was kept constant at 6. As shown, at a certain ferrate dose, e.g. 4 mg L^{-1}, the turbidity removal was increased with increasing initial turbidity. The maximum turbidity removal was observed in the

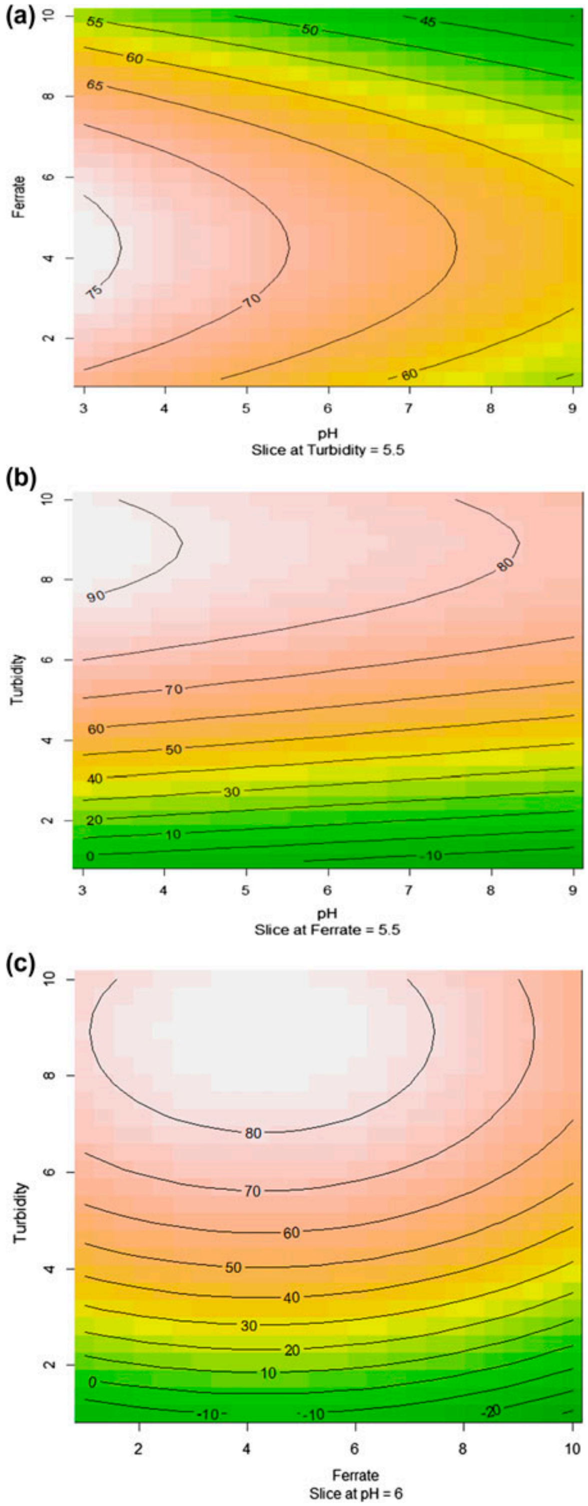

Fig. 4. Contour plots for the effect of (a) ferrate(VI) dose (mg L^{-1}) and coagulation pH, (b) turbidity (NTU) and coagulation pH, (c) turbidity (NTU) and ferrate(VI) dose (mg L^{-1}) on the turbidity removal.

Table 9
Experimental and predicted values of the responses at the optimal levels predicted by RSM

			Turbidity removal (%)	
pH	Turbidity (NTU)	Ferrate (mg/L)	Predicted	Experimental
3	8.89	4.26	94.65	89.04 ± 1.14
6.5	8.89	4.26	86.14	88.28 ± 0.93

initial turbidity higher than 7 NTU, while ferrate concentration ranged from 2 to 6 mg L^{-1}. In the entire ferrate(VI) dosage, minimum turbidity removal was reached when the initial turbidity was less than 2 NTU. It is worth noting that, at the initial turbidities lower than 5 NTU, increasing ferrate(VI) dosage up to 10 mg L^{-1} did not improve coagulation process, and the removal efficiency declined slightly, while at the initial turbidity higher than 5 NTU, increasing ferrate (VI) dosage showed reverse effect, especially at a dosage of 6–10 mg L^{-1}.

It is obvious from Fig. 4 that, ferrate(VI) coagulation performance is superior in turbidity removal in both acidic and neutral conditions. This is encouraging due to the fact that pH range in natural waters varies from 6 to 8; hence pH adjustment is not necessary for turbidity removal. In acidic conditions, hydrolysis of ferrate(VI) is seldom affected, and it seems that both adsorption and sweeping are the most probable mechanisms for turbidity removal. The findings of the study were in good agreement with [46]. The decrease in turbidity removal with ferrate(VI) at higher pH (above pH 8), might be attributed to the competition between hydroxyl ions and negatively charged colloidal particles [47]. Ferrate(VI) speciation in different pH values has been reported in [35]. It has shown that in the pH values lower than 6, ferrate(VI) decomposes to $Fe(OH)_3$ and the reaction occurs very swiftly, which seems to be the main reason for better coagulation/flocculation in this region (Eq. (1)), while in alkaline pH range ferrate(VI) is more stable and FeO_4^{2-} ion is present in the solution that decomposes slowly, which explains ferrate(VI) redox potential.

3.5. Process optimization and confirmation

To obtain the optimum jar test condition through the model equation predicted by RSM, the Solver "Add-ins" was applied using reasonable criteria. The criteria were maximum turbidity removal, ferrate(VI) dosage in the studied range (1–10 mg L^{-1}), and initial pH in the studied range (3–9). In the optimum conditions, all parameters simultaneously meet the predicted desirable criteria. Based on the assumptions noted, the predicted optimal conditions were: initial turbidity of 8.9 NTU, pH 3, and ferrate(VI) dosage of 4.26 mg L^{-1}, under which the maximum removal efficiency was estimated to be 94.65%. To confirm the validity of the results predicted by the model, additional laboratory experiments were conducted in four replicates. As can be seen in Table 9, experimental data were in good consistency with those predicted through the regression model. Also, there is another set of experiments shown in Table 9, which is the same as the above-mentioned optimal conditions except for initial pH. Initial pH of 6.5, as it is a common pH in surface waters, was tested with the other optimal conditions to determine whether the predicted results from the model are attainable. According to the results, both predicted and experimental data were in close agreement, and the most interesting finding was that there was no significant difference ($p = 0.4$) between the results obtained experimentally in both pH, which is very crucial from the operational point of view.

4. Conclusion

The experimental work showed that ferrate(VI), when used alone, was not successful in TCAA degradation. On the contrary, the results for turbidity removal were promising, and more than 95% removal was achieved, while TCAA contribution on the coagulation/flocculation performance was negligible, and 24% TCAA degradation was obtained. Therefore, another set of experiments was designed with only effective factors i.e. pH, initial turbidity, and modified ferrate dosage (1–10 mg L^{-1}), on turbidity removal.

The optimal operating point (initial turbidity: 8.89 NTU, pH 3, and initial ferrate(VI) dosage: 4.26 mg/L) giving maximum turbidity removal has been found using Solver "Add-ins" in Microsoft Excel 2010. Based on the ANOVA analysis R^2, R^2_{adj}, R^2_{pred}, and lack of fit values of regressions model equation were 0.915, 0.896, 0.849, and 0.26, respectively, ensuring a satisfactory adjustment of the quadratic regression model with the experimental data.

Under optimized conditions the experimental data confirmed the values predicted by the model, so it is clear that the RSM is a powerful and effective tool for optimizing the coagulation/flocculation process for turbidity removal.

Supplementary material

The supplementary material for this paper is available online at http://dx.doi.10.1080/19443994.2016.1147380.

Acknowledgments

The authors wish to thank Tehran University of Medical Sciences (TUMS) for supporting this work under Research Fund grant number 94-01-27-28256. The work was carried out in the laboratories of the department of Environmental Health Engineering.

References

[1] M.D. Esclapez, I. Tudela, M.I. Díez-García, V. Sáez, A. Rehorek, P. Bonete, J. González-García, Towards the complete dechlorination of chloroacetic acids in water by sonoelectrochemical methods: Effect of the anodic material on the degradation of trichloroacetic acid and its by-products, Chem. Eng. J. 197 (2012) 231–241.

[2] W. Lei, Z. Huifen, Y. Xin, Dechlorination and decomposition of trichloroacetic acid by glow discharge plasma in aqueous solution, Electrochim. Acta 115 (2014) 332–336.

[3] M.D. Esclapez, I. Tudela, M.I. Díez-García, V. Sáez, P. Bonete, Towards the complete dechlorination of chloroacetic acids in water by sonoelectrochemical methods: Effect of the cathode material on the degradation of trichloroacetic acid and its degradation by-products, Appl. Catal. B 166 (2015) 66–74.

[4] R. Chalatip, R. Chawalit, R. Nopawan, Removal of haloacetic acids by nanofiltration, J. Environ. Sci. 21 (2009) 96–100.

[5] U.E. ProtectionAgency, National primary drinking water regulations: Disinfectants and disinfection byproducts-final rule, Federal Register 63 (1998) 69390.

[6] M. Tomaszewska, S. Mozia, A.W. Morawski, Removal of organic matter by coagulation enhanced with adsorption on PAC, Desalination 161 (2004) 79–87.

[7] M. Yan, D. Wang, J. Qu, J. Ni, C.W. Chow, Enhanced coagulation for high alkalinity and micro-polluted water: The third way through coagulant optimization, Water Res. 42 (2008) 2278–2286.

[8] Z. Yang, B. Gao, Q. Yue, Coagulation performance and residual aluminum speciation of Al_2 $(SO_4)_3$ and polyaluminum chloride (PAC) in Yellow River water treatment, Chem. Eng. J. 165 (2010) 122–132.

[9] J. Nouri, A. Mahvi, E. Bazrafshan, Application of electrocoagulation process in removal of zinc and copper from aqueous solutions by aluminum electrodes, Int. J. Environ. Res. 4 (2010) 201–208.

[10] A.H. Mahvi, S.J.A.-D. Ebrahimi, A. Mesdaghinia, H. Gharibi, M.H. Sowlat, Performance evaluation of a continuous bipolar electrocoagulation/electrooxidation–electroflotation (ECEO–EF) reactor designed for simultaneous removal of ammonia and phosphate from wastewater effluent, J. Hazard. Mater. 192 (2011) 1267–1274.

[11] H. Zhao, C. Hu, H. Liu, X. Zhao, J. Qu, Role of aluminum speciation in the removal of disinfection byproduct precursors by a coagulation process, Environ. Sci. Technol. 42 (2008) 5752–5758.

[12] E.L. Sharp, S.A. Parsons, B. Jefferson, Seasonal variations in natural organic matter and its impact on coagulation in water treatment, Sci. Total Environ. 363 (2006) 183–194.

[13] Z.L. Yang, B.Y. Gao, Q.Y. Yue, Y. Wang, Effect of pH on the coagulation performance of Al-based coagulants and residual aluminum speciation during the treatment of humic acid–kaolin synthetic water, J. Hazard. Mater. 178 (2010) 596–603.

[14] E. Gauthier, I. Fortier, F. Courchesne, P. Pepin, J. Mortimer, D. Gauvreau, Aluminum forms in drinking water and risk of alzheimer's disease, Environ. Res. 84 (2000) 234–246.

[15] A. Becaria, D.K. Lahiri, S.C. Bondy, D. Chen, A. Hamadeh, H. Li, R. Taylor, A. Campbell, Aluminum and copper in drinking water enhance inflammatory or oxidative events specifically in the brain, J. Neuroimmunology 176 (2006) 16–23.

[16] G. Berthon, Aluminium speciation in relation to aluminium bioavailability, metabolism and toxicity, Coord. Chem. Rev. 228 (2002) 319–341.

[17] T. Waite, K. Gray, Oxidation and coagulation of wastewater effluent utilizing ferrate (VI) ion, Stud. Environ. Sci. 23 (1984) 407–420.

[18] X. Zhang, H. Lei, K. Chen, Z. Liu, H. Wu, H. Liang, Effect of potassium ferrate (K_2 FeO_4) on sludge dewaterability under different pH conditions, Chem. Eng. J. 210 (2012) 467–474.

[19] V. Sharma, Disinfection performance of Fe(VI) in water and wastewater: A review, Water Sci. Technol. 55 (2007) 225–232.

[20] V.K. Sharma, Potassium ferrate (VI): An environmentally friendly oxidant, Adv. Environ. Res. 6 (2002) 143–156.

[21] Y. Chen, Y. Xiong, Z. Wang, Y. Chen, G. Chen, Z. Liu, UV/ferrate (VI) oxidation of profenofos: efficiency and mechanism, Desalin. Water Treat. (2014) 1–8.

[22] J.-Q. Jiang, B. Lloyd, Progress in the development and use of ferrate (VI) salt as an oxidant and coagulant for water and wastewater treatment, Water Res. 36 (2002) 1397–1408.

[23] B.H. Bielski, V.K. Sharma, G. Czapski, Reactivity of ferrate (V) with carboxylic acids: a pre-mix pulse radiolysis study, Radiat. Phys. Chem. 44 (1994) 479–484.

[24] J. Rush, J. Cyr, Z. Zhao, B. Bielski, The oxidation of phenol by ferrate (VI) andferrate (V), Free Radical Res. 22 (1995) 349–360.

[25] M.D. Johnson, B.J. Hornstein, Unexpected selectivity in the oxidation of arylamines with ferrate–preliminary mechanistic considerations, Chem. Commun. (1996) 965–966.

[26] Q. Han, H. Wang, W. Dong, T. Liu, Y. Yin, H. Fan, Degradation of bisphenol a by ferrate (VI) oxidation:

Kinetics, products and toxicity assessment, Chem. Eng. J. 262 (2015) 34–40.

[27] K. Gray, T. Waite, Coagulation and precipitation studies of the ferrate (VI) ion, in: Abstracts of Papers of the American Chemical Society, American Chemical Society 1155 16th st, Nw, Washington, DC, 1983, 20036.

[28] J.-Q. Jiang, H. Durai, R. Winzenbacher, M. Petri, W. Seitz, Drinking water treatment by in situ generated ferrate (VI), Desalin. Water Treat. 55 (2014) 1–9.

[29] J.Q. Jiang, Advances in the development and application of ferrate (VI) for water and wastewater treatment, J. Chem. Technol. Biotechnol. 89 (2014) 165–177.

[30] J.-Q. Jiang, B. Lloyd, L. Grigore, Preparation and evaluation of potassium ferrate as an oxidant and coagulant for potable water treatment, Environ. Eng. Sci. 18 (2001) 323–328.

[31] M. Khayet, A. Zahrim, N. Hilal, Modelling and optimization of coagulation of highly concentrated industrial grade leather dye by response surface methodology, Chem. Eng. J. 167 (2011) 77–83.

[32] J.-P. Wang, Y.-Z. Chen, Y. Wang, S.-J. Yuan, H.-Q. Yu, Optimization of the coagulation-flocculation process for pulp mill wastewater treatment using a combination of uniform design and response surface methodology, Water Res. 45 (2011) 5633–5640.

[33] M. Domino, B. Pepich, D. Munch, P. Fair, Y. Xie, EPA Method 552.3, Revision 1.0: Determination of haloacetic acids and Dalapon in drinking water by liquid-liquid microextraction, derivatization, and gas chromatography with electron capture detection, 2003, EPA/815/B-03/002.

[34] B.H. Bielski, M. Thomas, Studies of hypervalent iron in aqueous solutions. 1. Radiation-induced reduction of iron (VI) to iron (V) by CO_2, J. Am. Chem. Soc. 109 (1987) 7761–7764.

[35] C. Li, X. Li, N. Graham, A study of the preparation and reactivity of potassium ferrate, Chemosphere 61 (2005) 537–543.

[36] A. Zahrim, A. Nasimah, N. Hilal, Coagulation/flocculation of lignin aqueous solution in single stage mixing tank system: Modeling and optimization by response surface methodology, J. Environ. Chem. Eng. 3 (2015) 2145–2154.

[37] J. Ma, W. Liu, Effectiveness and mechanism of potassium ferrate (VI) preoxidation for algae removal by coagulation, Water Res. 36 (2002) 871–878.

[38] K. Wang, J. Guo, M. Yang, H. Junji, R. Deng, Decomposition of two haloacetic acids in water using UV radiation, ozone and advanced oxidation processes, J. Hazard. Mater. 162 (2009) 1243–1248.

[39] M. Zainal-Abideen, A. Aris, F. Yusof, Z. Abdul-Majid, A. Selamat, S. Omar, Optimizing the coagulation process in a drinking water treatment plant–comparison between traditional and statistical experimental design jar tests, Water Sci. Technol. 65 (2012) 496–503.

[40] A.T. Nair, A.R. Makwana, M.M. Ahammed, The use of response surface methodology for modelling and analysis of water and wastewater treatment processes: A review, Water Sci. Technol. 69 (2014) 464–478.

[41] S.S. Moghaddam, M.A. Moghaddam, M. Arami, Coagulation/flocculation process for dye removal using sludge from water treatment plant: Optimization through response surface methodology, J. Hazard. Mater. 175 (2010) 651–657.

[42] S. Ghafari, H.A. Aziz, M.H. Isa, A.A. Zinatizadeh, Application of response surface methodology (RSM) to optimize coagulation–flocculation treatment of leachate using poly-aluminum chloride (PAC) and alum, J. Hazard. Mater. 163 (2009) 650–656.

[43] L. Guibai, J. Gregory, Flocculation and sedimentation of high-turbidity waters, Water Res. 25 (1991) 1137–1143.

[44] B. Shi, G. Li, D. Wang, C. Feng, H. Tang, Removal of direct dyes by coagulation: The performance of preformed polymeric aluminum species, J. Hazard. Mater. 143 (2007) 567–574.

[45] S.A. Muyibi, C.A. Okuofu, Coagulation of low turbidity surface waters with Moringa oleifera seeds, Int. J. Environ. Stud. 48 (1995) 263–273.

[46] J.-Q. Jiang, S. Wang, A. Panagoulopoulos, The exploration of potassium ferrate (VI) as a disinfectant/coagulant in water and wastewater treatment, Chemosphere 63 (2006) 212–219.

[47] Y. Zhao, B. Gao, H. Shon, B. Cao, J.-H. Kim, Coagulation characteristics of titanium (Ti) salt coagulant compared with aluminum (Al) and iron (Fe) salts, J. Hazard. Mater. 185 (2011) 1536–1542.